Published in final edited form as:
Biomaterials. 2010 November ; 31(32): 8254–8261. doi:10.1016/j.biomaterials.2010.07.041.

Perfusion and Characterization of an Endothelial Cell-Seeded Modular Tissue Engineered Construct Formed in a Microfluidic Remodeling Chamber

Omar F. Khan[1] and **Michael V. Sefton**[1]

[1] Department of Chemical Engineering and Applied Chemistry and the Institute of Biomaterials and Biomedical Engineering, University of Toronto

Abstract

Tissue engineered constructs containing tortuous endothelial cell-lined perfusion channels were formed by randomly assembling endothelial cell-seeded submillimeter-sized collagen cylinders (modules) into a microfluidic perfusion chamber. The interconnected void space produced by random module packing created flow channels that were lined with endothelial cells. The effect of perfusion (0.5 mL min^{-1}, Re^* = 14.36 and shear stress = 0.64 dyn cm^{-2}) through the tortuous channels on construct remodeling and endothelium quiescence was studied. Over time, modules fused at their points of contact and as they contracted, decreased the internal void space, which reduced the overall perfusion through the construct. As compared to static controls, perfusion caused a transient increase in activation (ICAM-1 and VCAM-1 expression) after 1 hour followed by a decrease after 24 hours. Proliferation (by BrdU) was reduced significantly, while KLF2, which is upregulated with atheroprotective laminar shear stress, was upregulated significantly after 24 hours. VE-cadherin became discontinuous and was significantly downregulated after 24 hours, which was likely caused by the dismantling of the endothelial cell adherens junctions during remodeling. Collectively, these outcomes suggest that flow through the construct did not drive the endothelial cells towards an inflamed, “atherosclerotic like” disturbed flow pathology.

Introduction

An artificial vascularized organ can be assembled from modular, submillimeter-sized cylinders that are randomly assembled into a larger container [1]. Modular rods made from collagen contain functional cells while the outside surface is seeded with endothelial cells (Figure 1a). The outer endothelial cell layer is expected to exhibit a non-thrombogenic blood-contacting surface [1], provided the cells maintain a non-activated phenotype. Random packing of modules in a container creates a network of endothelial cell-lined interconnected channels that enables blood perfusion (Figure 1b). These interconnected channels are tortuous and can contain curves, branches, contractions and expansions, which may lead to flow separation [2]. Flow separation, also known as disturbed flow, has long been known to cause endothelial

Correspondence to: Michael V. Sefton.

Postal Addresses: Omar F. Khan, Centre for Cellular and Biomolecular Research, 160 College Street, Room 440, Toronto, Ontario M5S 3E1 Canada, Phone: 1-416-978-6518, Fax: 1-416-978-8287, of.khan@utoronto.ca
Michael V. Sefton, Institute of Biomaterials and Biomedical Engineering, University of Toronto, 164 College Street, Suite 407, Toronto, Ontario M5S 3G9, Canada, Phone: 1-416-978-3088, Fax: 1-416-978-4317, michael.sefton@utoronto.ca

cell activation in large-diameter blood vessels *in vivo* [3] and so is a critical issue that requires investigation and resolution [4].

The non-thrombogenic, quiescent phenotype of endothelial cells and the successful perfusion of the construct are critical to the success of this tissue-engineered organ [5]. Many conditions, including fluid shear stress, basement membrane composition and the presence of smooth muscle cells have been implicated in the maintenance of the desired endothelial cell phenotype [6]. The type of flow and shear stress experienced by endothelial cells in a tissue engineered construct can have a large impact on phenotype. For example, laminar flow and steady shear stress can reduce activation, increase nitric oxide production, inhibit apoptosis and inhibit atherogenesis events such as vascular smooth muscle cell overgrowth [7–10]. In contrast, disturbed and non-laminar flow can cause the endothelium to become proinflammatory. These conditions can negatively influence the inflammatory, vasoreactive and oxidative states of the endothelium and lead to atherosclerotic plaque formation in vessels[11–15].

Microfluidics is used here to better study the myriad of conditions that may be necessary for the formation of functional tissue using the modular approach. We use a microfluidic-inspired remodeling chamber where modules are loaded in a microfluidic device to create a packed bed reactor and subjected to perfusion. A similar device was created by Bruzewicz et al [16]. We hypothesized that the shear stress (and mechanical loading) produced by perfusion will promote module remodeling and create vasculature-like channels that will self-optimize to best support surface-attached endothelial cell and embedded functional cells. Moreover, we hypothesized that the endothelium will maintain a quiescent phenotype despite the irregular flow through the tortuous vessel network created by the modular tissue-engineering approach [4]. The presented work focuses on the design, development and characterization of a remodeling chamber and the tissues produced therein. This initial work has been done with a view to characterizing the system before increasing the complexity of the modules through the addition of embedded therapeutic cells.

Materials and Methods

Chamber Fabrication

Microfluidic chambers (Figure 2a) were fabricated following the general rapid prototyping, molding and sealing steps outlined by Duffy et al [17]. Briefly, Goldline plain glass microscope slides (3″ × 1″, VWR International, Mississauga, ON) were cleaned and dehydrated. A seeding layer of SU-8 25 photoresist (MicroChem Corp, Newton, Massachusetts) was spin coated, soft baked, UV-exposed, and cured in a post-exposure bake. A second photoresist layer of SU-8 2150 was spin coated and soft baked. A photomask of the remodeling chamber was used in the UV exposure step, followed by a post-exposure bake. Masters were developed in SU-8 Developer Solution (MicroChem Corp) with agitation from a Heidolph Rotamax 120 orbital shaker (Heidolph Instruments GmbH & Co. KG, Schwabach, Germany) and hard baked. Average feature thickness (see Figure 2a) was 375 μm ± 88 μm. Masters were covered with Sylgard® 184 silicone elastomer (PDMS, Dow Corning Corporation, Midland, MI) and degassed under vacuum (25 inch Hg or ~93,000 Pa absolute). Due to the high aspect ratio of the pillars, air bubbles became trapped within them and so cycling between atmospheric and vacuum pressure was necessary to effectively remove all bubbles. PDMS was cured in a leveled oven at 75°C for 2 hours. Inlet and outlet port holes were punched into the PDMS mold which was then bonded to a 24 mm × 60 mm cover glass (Corning Life Sciences, Wilkes Barre, PA) after a 90 second plasma treatment (PDC-32G Plasma Cleaner, Harrick Scientific, Ossining, NY). After 30 minutes at rest, the bonded units were steam autoclaved for 30 minutes followed by 15 minutes of drying time to improve the PDMS-cover glass bond [18]. Female luer threads (Cole-Parmer Instrument Company, Vernon Hills, Il) were inserted into the inlet and outlet

holes and bonded using 5 Minute Epoxy (Devcon, Danvers, MA) to facilitate chip-to-world tubing connections. Assembled devices were ethylene oxide gas sterilized before use.

Flow Circuit Construction

Remodeling chambers were connected to a multichannel peristaltic pump and cell culture medium was circulated through the chamber in a closed loop as described elsewhere [4]. Each flow chamber had a corresponding static control that was not subjected to flow. At the desired time point, circuits were removed from their flow circuit and, along with their corresponding static controls, analyzed as described below.

Module Fabrication and Culture

Modules were fabricated according to the protocol of McGuigan et al [1]. Briefly, primary Human Umbilical Vein Endothelial Cells (HUVEC, Lonza, Basel, Switzerland) were cultured in EGM-2 medium (Lonza). Between passage 2 and 6, HUVEC were seeded on the surface of empty collagen modules. One day following module fabrication and cell seeding, modules were loaded into the remodeling chambers.

Remodeling chambers were primed with EGM-2 medium and filled with modules using a 5 mL syringe connected to the chamber's inlet luer lock (Figure 2b). Once the modules settled to the bottom of the syringe, they were pushed into the chamber and packed against the retaining wall. Flow circuit medium reservoirs were filled with 13 mL of culture medium and lines were primed to remove any air bubbles. Remodeling chambers were connected to the flow circuits and perfused at 0.5 mL min^{-1} for 1, 2, 24 or 48 hours.

Confocal Imaging

At the desired time points, the modular beds within the remodeling chambers were perfused with 4% paraformaldehyde (EMS, Fort Washington, PA) and stained for VE-cadherin, KLF2, ICAM-1 or VCAM-1, as described elsewhere [4].

For proliferation studies, a 2 hour pulse of the thymidine analog 5-bromo-2-deoxyuridine (10 μM, BrdU, Sigma, Oakville, ON) was used to label DNA synthesis in proliferating HUVEC. Cells were washed in PBS, fixed in 4% paraformaldehyde for 20 minutes, washed and permeablized with 0.2% Triton X-100 (Sigma). Cells were denatured with 2N HCl (Sigma) for 20 minutes, washed and remaining acid was neutralized with 0.1 M sodium borate (Sigma). BrdU was labeled by incubating for 1 hour in a 1:50 dilution of Alexa Fluor™ conjugated mouse monoclonal IgG anti-BrdU antibody (Molecular Probes). Hoechst nuclear stain (bisBenzimide H 33342 trihydrochloride, 1:100 dilution, Sigma-Aldrich) was used as a nuclear counter stain and as an indication of overall cell attachment.

Image and statistical analysis

Using the same confocal microscope settings (objective, gain and offset), each remodeling chamber and its corresponding static control were imaged. ImageJ macros were written to count the number of cells (nuclei) found in each image and to quantify marker expression (integrated density value, IDV). IDV was normalized by cell number (dividing IDV by the number of observed nuclei).

Q-Q plots were used to determine if data were normally distributed. For normally distributed data, independent sample means were compared using the student t-test and ANOVA with the Tukey HSD multiple-comparison correction. For data that was not normally distributed, independent sample means were compared using the non-parametric Wilcoxon Rank Sum test. Differences were considered statistically significant if $p < 0.05$.

Flow Characterization

To determine the Reynolds number within the remodeling chamber, the equation for packed bed reactors, Equation 1, was employed.

$$\mathrm{Re}^{*}=\frac{d_m U_s \rho_f}{\mu(1-\varepsilon)} \tag{1}$$

In Equation 1, ρ_f is the fluid density (assumed equal to water at 37°C), ε is the porosity of the packed module bed (estimated to be 0.64 based on image analysis using ImageJ), μ is the fluid viscosity (assumed equal to water at 37°C), ϕ is the sphericity factor of the modules (0.492, based on image analysis) and d_m is the diameter of a sphere with the same volume as a module (an average value 1.623 mm, based on image analysis). U_s is the superficial velocity. Flow was considered laminar when $Re^* < 10$ and turbulent when $Re^* > 2000$ [19].

The average shear stress within the remodeling chamber, τ^*, was estimated through the use of Equation 2, a modified Ergun equation [1,20].

$$\tau^{*}=\frac{37.5(1-\varepsilon)\mu U_s}{\varepsilon^2 \varphi d_m} \tag{2}$$

Because modular beds were continually remodeling, the Reynolds number and average shear stress changed over time. Thus, the reported value of Re^* and τ^* are the initial values for the packed module bed.

Results

Remodeling chamber design

The remodeling chamber was designed as a PDMS-based microfluidic chip. The chip contained a long open space into which modules were loaded. Under flow, modules were pushed against a retaining wall near the outlet of the chamber and packed together (Figure 2). The size, number and spacing of the retaining pillars were optimized to produce the lowest pressure drop across the system. Initially, several consecutive walls of retaining pillars closely packed together were used, but in this case the resulting pressure drop was large enough to ultimately lead to pressure buildup upstream of the modules. Because the modules were soft and compressible, they were deformed and forced through the retaining walls. By minimizing the number of and maximizing the void space between pillars, a stable packed module bed was achieved without excessive module deformation and loss. This also reduced the amount of channeling through the packed module bed that would occur if the modules were to be washed out of the chamber, creating a free-flowing channel. Such channels reduce fluid perfusion through the packed bed.

After 1 hour (at a flowrate of 0.5 mL min^{-1}; nominal $Re^* = 14.36$ and shear stress = 0.64 dyn cm^{-2}) modules began to compact and fuse together as shown in Figure 3. Over time, pores were observed to decrease in size and some would collapse fully. As pores decreased in size, channeling through larger channels, the top surface of the bed and along the chamber side walls increased. This meant that only the cells lining the large channels and the perimeter of the modular bed were experiencing fluid shear.

The initial Reynolds number (14.36) lies in the transition zone between laminar and turbulent flow. Because flow was not completely laminar, this indicated an increasing probability of

irregularities forming, such as increased flow separation and the concordant vortex formation, which are hallmarks of disturbed flow. Moreover, the continual remodeling resulted in porosity (ε) changes. As time progressed, the porosity of the packed bed decreased as modules were compacted and fused together. This decreased flow through the less porous regions and change the actual Re^* and τ^*.

Endothelial cell behaviour

Modules subject to flow in the remodeling chamber and corresponding static controls were stained for VE-cadherin and KLF2 (Figure 4a). For VE-cadherin, no significant differences in normalized expression (fluorescent signal relative to the number of nuclei) between the static and flow cases were found at the 1 hour time point but at 24 hours, there was less expression with perfusion ($p = 0.018$, Figure 5a). Furthermore, the quality of the VE-cadherin was different. As seen in Figure 4a, VE-cadherin expression in static controls appeared as a solid, continuous line around the perimeter of the cells. After 1 hour of perfusion, sections of the continuous perimeter line were gone and appeared as a dashed line in other regions. After 24 hours of perfusion, the expression became increasingly discontinuous and disorganized. VE-cadherin was no longer confined to a line around the cell perimeter but was seen throughout the cell, including around nuclei and cytoplasm. Though the average KLF2 expression was higher with perfusion at both time points, only the 24 hour difference was statistically significant ($p = 0.017$, Figure 5b). Modules were also stained for ICAM-1 and VCAM-1 after 1 and 24 hours (Figure 4b). As shown in Figure 6a, the average expression of ICAM-1 was higher with perfusion after 1 hour but became lower with perfusion after 24 hours while Figure 6b shows a lower amount of VCAM-1 with perfusion at both time points. However, unlike VE-cadherin and KLF2, these differences were not statistically significant.

In disturbed flow, confluent monolayers of HUVEC become proliferative [21]. Hence, we assessed the amount HUVEC proliferation by BrdU uptake as an indicator of endothelium quality (Figure 7). Both the outer (edge) and inner (core) regions of the module bed were examined because, due to the ongoing remodeling of the modular tissue, areas closest to the remodeling chamber's walls were often observed to experience the greatest amount of channeling (fluid bypassing through these regions) while the flow through the centre region of the tissue reduced as modules compacted and fused, reducing porosity. Two hours after confluent modules were loaded into the remodeling chamber, no statistically significant differences in the levels of proliferation were seen between the flow and static cases. However, after 24 hours, proliferation in the flow cases decreased ($p < 0.001$) while static cases remained relatively high. By the 48^{th} hour, there were again no statistically significant differences in proliferation between flow and static controls as proliferation within the static controls decreased to a level similar to that of the flow case. While the amount of proliferation in static cases eventually decreased from its initial high, perfusion was able to achieve and maintain this reduction 24 hours sooner.

Discussion

We describe a microfluidic device that is used to mimic the remodeling that occurs when endothelialized modules are subjected to flow. Several microfluidic devices have been developed to culture three-dimensional constructs in conjunction with some form of perfusion for both tissue engineering and pharmacological diagnostic purposes. For example, cell-embedded collagen modules were assembled into a microfluidic channel and perfused at low flow rates [16]. Intended for toxicological screening, a PDMS-based microchamber was used to incubate and perfuse precision-cut liver slices [22]. A hybrid collagen gel and PDMS device that facilitated perfusion was used to create an epithelial and karatocyte corneal tissue bilayer construct [23] while an aerated perfusion platform was used to form and maintain neural-

astrocytic constructs made from matrigel [24]. Poly(glycerol sebacate), a biodegradable elastomer, was used to create single-layer microfluidic networks that were stacked and bonded to create three-dimensional scaffold networks which were seeded with hepatocyte cells and perfused [25]. Another method encapsulated micromolded meshes of gelatin in a cell-containing hydrogel such as collagen or fibrinogen. The gelatin mesh was later removed by heating and flushing, leaving behind interconnected channels within the hydrogel. The channels withstood perfusion and could also be seeded with endothelial cells [26].

Our intent was to create a chamber that allowed us to follow the changes in endothelial phenotype over time and to compare the effects of flow to the static culture case, with actual modules rather than endothelial cells attached to a fibronectin coated cover glass [4]. In a previous report, a two-dimensional microfluidic device which reproduced the endothelial cell-lined tortuous channels found within the modular bed was used to examine the effect of perfusion on endothelial cell phenotype. We found that higher levels of flow was sufficient to reduce ICAM-1 and VCAM-1 expression in many disturbed flow-prone channels that contained branches, curves, expansions and contractions. VE-cadherin expression was also reduced and became discontinuous in all channels and KLF2 was found to be largely independent of shear stress. Furthermore, areas where multiple channels converged were found to be the most prone to leukocyte attachment.

In this report, a full three-dimensional module bed was constructed and subjected to perfusion. To characterize the flow within the module bed, the system was modeled as a packed bed of particles and the Re^* and τ^* were calculated. The assumptions used in this model were that the packed bed was equivalent to many tubes of equivalent diameter following tortuous paths of equal length, all carrying fluid with a similar velocity [19]. Owing to the ongoing remodeling of the module bed, the channels and flow field were constantly evolving and so computed Re^* and τ^* values were only valid for the initial system.

The module bed was perfused at a relatively low flowrate because the maximum flowrate of the system was limted by the collagen gel modules' low modulus. Higher flowrates compacted, deformed and, at times, washed the modules out of the remodeling chamber. Nonetheless, even at the low shear the modules remodeled over time (Figure 3) such that many channels collapsed leading to channeling around the aggregate of modules or through larger channels. As it remodeled, the bed's porosity decreased and the shear stress in the areas that experienced channeling likely increased due to the greater amount of fluid passing through those areas.

Moreover the reduced flow through the diminishing channels likely affected the endothelial cells in those channels. In animals, the volume of flow through blood vessels has been shown to influence the size of blood vessels. When the blood flow through the carotid arteries of rabbits was restricted, the diameters of denuded arteries remained the same while those with intact endothelium responded by concordantly reducing vessel diameter by acting on the surrounding smooth muscle cells [27]. A similar mechanism may occur in this system if smooth muscle cells (or the equivalent) were to be added to the modules. Alternatively, endothelial cells may, over the longer term, migrate towards or preferentially proliferate in the regions where flow is higher (areas of channeling) in order to take advantage of the superior rates of transport. The onset of channeling may also appear to be similar to vessel growth in arteriogenesis. In arteriogenesis, new vessel formation is not induced by hypoxia but instead by physical forces including flow and shear stress [28]. The larger interconnected interstices, similar to anastomoses, expand to form fluid bypasses. This flow associated remodeling mimics the remodeling that occurs *in vivo* in module implants [29], although there is no host response and the flow field is different in the remodeling chamber. This is likely to prove a key advantage of the remodeling chamber as it enables the study of remodeling under complex conditions but with greater, albeit imperfect, control than the *in vivo* situation. A challenge for the future is

to create a remodeling chamber that combines the well defined flow field of a planar laminar flow chamber with the biological complexity of remodeling.

Endothelial cell behaviour

Under laminar flow conditions, VE-cadherin is expressed around the perimeter of endothelial cells in a continuous fashion, but in the presence of disturbed flow, its distribution becomes broken and discontinuous [30]. In previous work where the tortuous channels from a single, two-dimensional plane within a three-dimensional modular construct were modeled and the effect of flow through these channels on endothelial cells was examined, the amount of VE-cadherin expression was unaffected by low flowrates and downregulated by higher ones. Moreover, discontinuous VE-cadherin was noted and was attributed to the consequences of disturbed flow in the two-dimensional flow system [4]. Although we observed a downregulation in expression after 24 hours ($p = 0.018$), and broken and discontinuous VE-cadherin expression, we believe it is not due to disturbed flow. Instead we attribute the discontinuous VE-cadherin to the endothelial cell reorientation and remodeling process. When endothelial cells are exposed to shear stress after being statically cultured, their continuous VE-cadherin expression temporarily becomes disorganized as they re-align with the flow [31]. Moreover, during endothelial cell migration, VE-cadherin decreases in intensity at the cell's leading edge [32].

These VE-cadherin results highlight the major caveat of this system: due to the on-going remodeling of the construct, endothelial cells may experience prolonged periods of discontinuous VE-cadherin. Discontinuous, diffusely distributed VE-cadherin has been shown to increase the permeability of the endothelium to high molecular weight molecules, increase transendothelial migration and even result in exposed basement membrane [33,34]. Once implanted, this may potentiate a foreign body reaction and host response beyond the one caused by an increase in activation alone (*i.e.* upregulated ICAM-1 and VCAM-1).

In contrast to the VE-cadherin results, the BrdU proliferation and ICAM-1/VCAM-1 activation data showed that tortuous flow through the packed module bed was not detrimental to the confluent, surface-attached endothelial cells. Perfusion was able to significantly reduce the amount of endothelial cell proliferation 24 hours earlier that static controls. Though not statistically significant, the average ICAM-1 levels with perfusion were slightly higher than static controls at 1 hour and lower at 24 hours while VCAM-1 showed a slight decrease at both time points. Moreover, these results appeared to agree with the activation data from our previous two-dimensional model work which showed that activation (relative to static controls) was unaffected by low flow rates and reduced by higher ones. A temporary increase in endothelial cell proliferation and activation is a normal response since the application of shear is known to cause a transient increase of pro-inflammatory and proliferative pathways, which become downregulated when the directed shear is sustained [35]. Perhaps these observations suggest that the modular tissue requires pre-conditioning with shear until transient responses subside. This may help reduce the amount of leukocyte recruitment into the modular tissue following implantation.

KLF2 observations also showed that perfusion was beneficial to the modular system. KLF2, a transcription factor, is induced by laminar shear stress in cultured HUVEC [36]. Here, after 24 hours, flow caused an upregulation in KLF2 ($p = 0.017$). The increased KLF2 expression is ultimately advantageous to the *in vivo* survival of the modular construct because it can reduce thrombogenicity (by inducing thrombomodulin and endothelial nitric oxide synthase, and by reducing plasminogen activator inhibitor-1 expression) and inhibit the induction of VCAM-1 and E-selectin [36–38].

In this work modules were empty; that is, there were no cells embedded within the collagen. Since the presence of embedded cells such as mesenchymal stem cells dramatically alters the remodeling process and endothelial cell phenotype the next step is to add such cells (and the additional complexity) to the remodeling chamber.

Conclusions

When creating vascularized tissue constructs, the health of the endothelium is of paramount concern. A non activated, quiescent endothelium reduces the host response to the implanted construct while enabling blood flow and the provision of nutrients and waste removal for the therapeutic cells within the construct. The perfusion channels created within our randomly assembled construct were tortuous in nature, leading to concerns that the flow could drive the construct's endothelium towards an inflamed, atherosclerotic-like pathology. However, we have shown that perfusion does not appear to significantly increase activation. Moreover, the observed increase in KLF2 expression may suggest that flow through the construct was beneficial to the endothelial cells. Future work will examine the performance of increasingly complex constructs that embed functional, therapeutic cells within the modules.

Acknowledgments

The authors acknowledge the financial support of the Natural Sciences and Engineering Research Council, the Canadian Institutes of Health Research and the US National Institutes of Health (EB006903). O.F. Khan acknowledges scholarship support from the Ontario Graduate Scholarship Program.

References

1. McGuigan AP, Sefton MV. Vascularized organoid engineered by modular assembly enables blood perfusion. Proc Natl Acad Sci U S A 2006;103:11461–11466. [PubMed: 16864785]
2. Chang, PK. Separation of flow. Oxford: Pergamon Press; 1970.
3. Cunningham KS, Gotlieb AI. The role of shear stress in the pathogenesis of atherosclerosis. Lab Invest 2005;85:9–23. [PubMed: 15568038]
4. Khan OF, Sefton MV. Endothelial cell behaviour within a microfluidic mimic of the flow channels of a modular tissue engineered construct. Biomed Microdevices. 2010 Submitted.
5. McGuigan AP, Sefton MV. The thrombogenicity of human umbilical vein endothelial cell seeded collagen modules. Biomaterials 2008;29:2453–2463. [PubMed: 18325586]
6. Imberti B, Seliktar D, Nerem RM, Remuzzi A. The response of endothelial cells to fluid shear stress using a co-culture model of the arterial wall. Endothelium 2002;9:11–23. [PubMed: 12901357]
7. Cucina A, Sterpetti AV, Borrelli V, Pagliei S, Cavallaro A, D'Angelo LS. Shear stress induces transforming growth factor-beta1 release by arterial endothelial cells. Surgery 1998;123:212–217. [PubMed: 9481408]
8. De Caterina R, Libby P, Peng HB, Thannickal VJ, Rajavashisth TB, Gimbrone J, et al. Nitric oxide decreases cytokine-induced endothelial activation. Nitric oxide selectively reduces endothelial expression of adhesion molecules and proinflammatory cytokines. J Clin Invest 1995;96:60–68. [PubMed: 7542286]
9. Dimmeler S, Haendeler J, Rippmann V, Nehls M, Zeiher AM. Shear stress inhibits apoptosis of human endothelial cells. FEBS Lett 1996;399:71–74. [PubMed: 8980122]
10. Kubes P, Suzuki M, Granger DN. Nitric oxide: An endogenous modulator of leukocyte adhesion. Proc Natl Acad Sci U S A 1991;88:4651–4655. [PubMed: 1675786]
11. Walpola PL, Gotlieb AI, Cybulsky MI, Langille BL. Expression of ICAM-1 and VCAM-1 and monocyte adherence in arteries exposed to altered shear stress. Arterioscler Thromb Vasc Biol 1995;15:2–10. [PubMed: 7538423]
12. Hsiai TK, Cho SK, Wong PK, Ing M, Salazar A, Sevanian A, et al. Monocyte recruitment to endothelial cells in response to oscillatory shear stress. FASEB J 2003;17:1648–1657. [PubMed: 12958171]

13. Chappell DC, Varner SE, Nerem RM, Medford RM, Alexander RW. Oscillatory shear stress stimulates adhesion molecule expression in cultured human endothelium. Circ Res 1998;82:532–539. [PubMed: 9529157]

14. Asakura T, Karino T. Flow patterns and spatial distributions of atherosclerotic lesions in human coronary arteries. Circ Res 1990;66:1045–1066. [PubMed: 2317887]

15. Passerini AG, Polacek DC, Shi C, Francesco NM, Manduchi E, Grant GR, et al. Coexisting proinflammatory and antioxidative endothelial transcription profiles in a disturbed flow region of the adult porcine aorta. Proc Natl Acad Sci U S A 2004;101:2482–2487. [PubMed: 14983035]

16. Bruzewicz DA, McGuigan AP, Whitesides GM. Fabrication of a modular tissue construct in a microfluidic chip. Lab Chip 2008;8:663–671. [PubMed: 18432334]

17. Duffy DC, McDonald JC, Schueller OJA, Whitesides GM. Rapid prototyping of microfluidic systems in poly(dimethylsiloxane). Anal Chem 1998;70:4974–4984.

18. McDonald JC, Whitesides GM. Poly(dimethylsiloxane) as a material for fabricating microfluidic devices. Acc Chem Res 2002;35:491–499. [PubMed: 12118988]

19. Rhodes, M. Introduction to particle technology. 2. Chichester, England; Hoboken, NJ: John Wiley & Sons, Ltd; 2008.

20. McGuigan AP, Sefton MV. Design criteria for a modular tissue-engineered construct. Tissue Eng 2007;13:1079–1089. [PubMed: 17439395]

21. Tardy Y, Resnick N, Nagel T, Gimbrone J, Dewey J. Shear stress gradients remodel endothelial monolayers in vitro via a cell proliferation-migration-loss cycle. Arterioscler Thromb Vasc Biol 1997;17:3102–3106. [PubMed: 9409299]

22. Van Midwoud PM, Groothuis GMM, Merema MT, Verpoorte E. Microfluidic biochip for the perifusion of precision-cut rat liver slices for metabolism and toxicology studies. Biotechnol Bioeng 2010;105:184–194. [PubMed: 19718695]

23. Puleo CM, McIntosh Ambrose W, Takezawa T, Elisseeff J, Wang TH. Integration and application of vitrified collagen in multilayered microfluidic devices for corneal microtissue culture. Lab Chip 2009;9:3221–3227. [PubMed: 19865728]

24. Vukasinovic J, Cullen DK, Laplaca MC, Glezer A. A microperfused incubator for tissue mimetic 3D cultures. Biomed Microdevices 2009;11:1155–1165. [PubMed: 19562488]

25. Bettinger CJ, Weinberg EJ, Kulig KM, Vacanti JP, Wang Y, Borenstein JT, et al. Three-dimensional microfluidic tissue-engineering scaffolds using a flexible biodegradable polymer. Adv Mater 2006;18:165–169. [PubMed: 19759845]

26. Golden AP, Tien J. Fabrication of microfluidic hydrogels using molded gelatin as a sacrificial element. Lab Chip 2007;7:720–725. [PubMed: 17538713]

27. Langille BL, O'Donnell F. Reductions in arterial diameter produced by chronic decreases in blood flow are endothelium-dependent. Science 1986;231:405–407. [PubMed: 3941904]

28. Heil M, Eitenmuller I, Schmitz-Rixen T, Schaper W. Arteriogenesis versus angiogenesis: Similarities and differences. J Cell Mol Med 2006;10:45–55. [PubMed: 16563221]

29. Chamberlain MD, Gupta R, Sefton MV. Chimeric vessel tissue engineering driven by endothelialized modules. Tissue Eng. 2010 Submitted.

30. Miao H, Hu YL, Shiu YT, Yuan S, Zhao Y, Kaunas R, et al. Effects of flow patterns on the localization and expression of VE-cadherin at vascular endothelial cell junctions: In vivo and in vitro investigations. J Vasc Res 2005;42:77–89. [PubMed: 15637443]

31. Noria S, Cowan DB, Gotlieb AI, Langille BL. Transient and steady-state effects of shear stress on endothelial cell adherens junctions. Circ Res 1999;85:504–514. [PubMed: 10488053]

32. Lampugnani MG, Corada M, Caveda L, Breviario F, Ayalon O, Geiger B, et al. The molecular organization of endothelial cell to cell junctions: Differential association of plakoglobin, β-catenin, and alpha-catenin with vascular endothelial cadherin (VE-cadherin). J Cell Biol 1995;129:203–217. [PubMed: 7698986]

33. Corada M, Mariotti M, Thurston G, Smith K, Kunkel R, Brockhaus M, et al. Vascular endothelial-cadherin is an important determinant of microvascular integrity in vivo. Proc Natl Acad Sci U S A 1999;96:9815–9820. [PubMed: 10449777]

34. Hordijk PL, Anthony E, Mul FPJ, Rientsma R, Oomen LCJM, Roos D. Vascular-endothelial-cadherin modulates endothelial monolayer permeability. J Cell Sci 1999;112:1915–1923. [PubMed: 10341210]

35. Chien S. Effects of disturbed flow on endothelial cells. Ann Biomed Eng 2008;36:554–562. [PubMed: 18172767]

36. SenBanerjee S, Lin Z, Atkins GB, Greif DM, Rao RM, Kumar A, et al. KLF2 is a novel transcriptional regulator of endothelial proinflammatory activation. J Exp Med 2004;199:1305–1315. [PubMed: 15136591]

37. Parmar KM, Larman HB, Dai G, Zhang Y, Wang ET, Moorthy SN, et al. Integration of flow-dependent endothelial phenotypes by Kruppel-like factor 2. J Clin Invest 2006;116:49–58. [PubMed: 16341264]

38. Dekker RJ, Boon RA, Rondaij MG, Kragt A, Volger OL, Elderkamp YW, et al. KLF2 provokes a gene expression pattern that establishes functional quiescent differentiation of the endothelium. Blood 2006;107:4354–4363. [PubMed: 16455954]

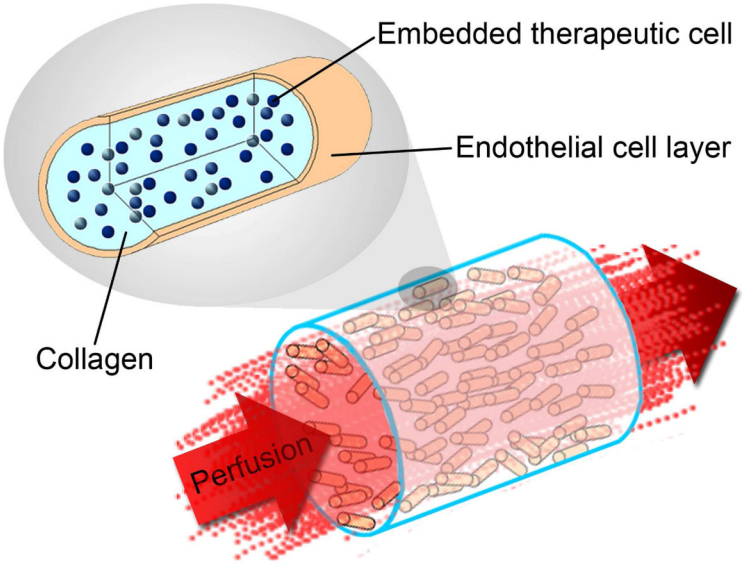

Figure 1.
Modular tissue engineering. Modular, sub-millimeter-sized cylinders are made from collagen with embedded functional cells and surface-attached endothelial cells. The random packing of modular cylinders in a larger container forms interconnecting channels lined with endothelial cells that allow for blood perfusion.

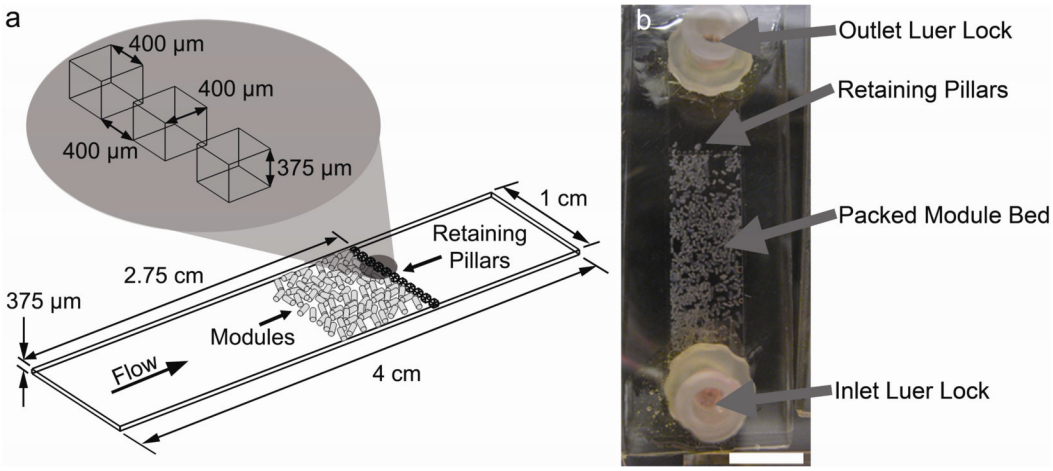

Figure 2.

(a) Remodeling chamber specifications. Modules were loaded within the chamber and under flow, packed against a retaining wall composed of pillars. Packed beds were 1 to 2 modules in thickness and the initial packed bed depth was approximately 2.5 mm. (b) Modules as they appeared immediately after loading and before settling. Scale bar = 1 cm.

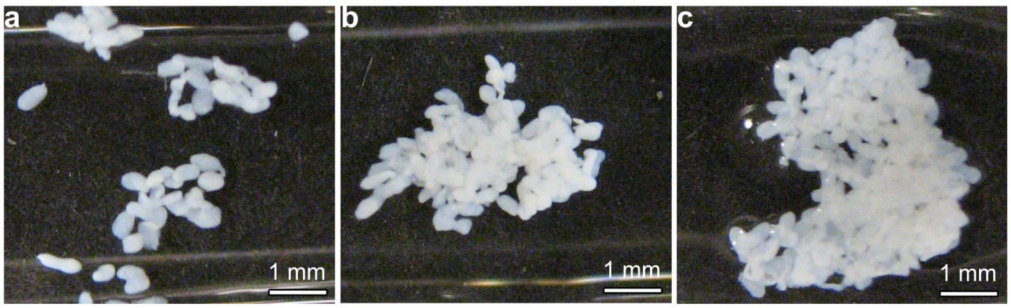

Figure 3.

HUVEC-seeded collagen modules removed from remodeling chambers after 2 (a), 24 (b) and 48 (c) hours of perfusion at a flow rate of 0.5 mL min^{-1}. Over the 48 hour period, modules began to fuse at their points of contact and compact to form a denser, less permeable mass. Scale bar = 1 mm.

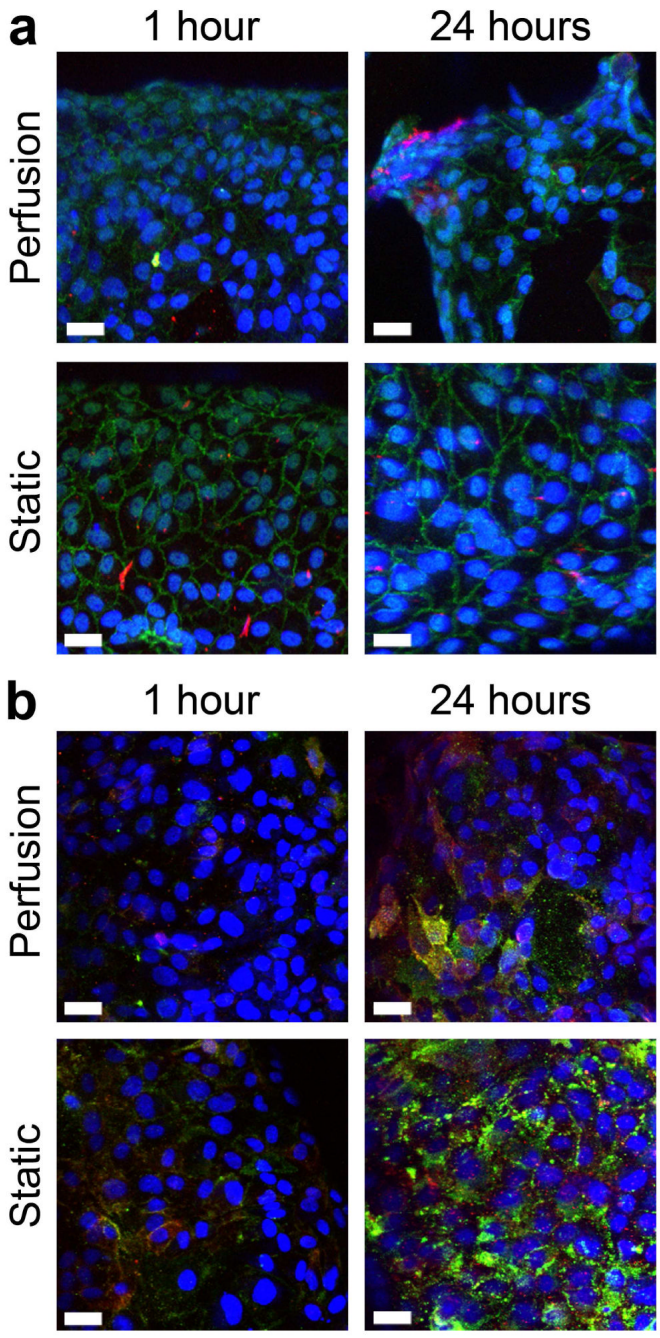

Figure 4.
Phenotype of HUVEC on modules within the remodeling chamber. (a) VE-cadherin (green) and KLF2 (red) expression. In many cases, KLF2 expression appeared to increase with flow. VE-cadherin in static controls appeared continuous around the perimeter of cells; however, with perfusion, expression around the cell perimeter was discontinuous and, at 24 hours, was seen throughout the cell. (b) HUVEC activation was determined by ICAM-1 (red) and VCAM-1 (green) staining. Several flow cases showed lower ICAM-1 and VCAM-1 expression, but these results were not statistically significant. Scale bars are 10 μm.

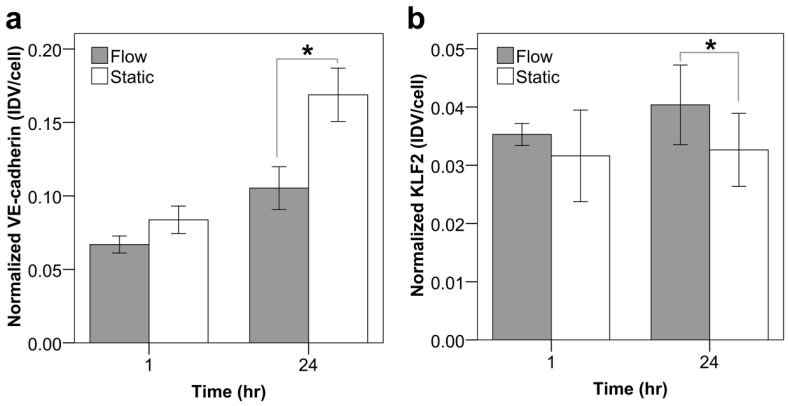

Figure 5.

VE-cadherin and KLF2 expression of endothelial cells on module surfaces through confocal microscopy and image analysis. The IDV for each marker was normalized to the total number of nuclei. The VE-cadherin signal only describes the total expression and not its quality or organization. (a) Flow appeared to cause a slight reduction in average VE-cadherin expression after 1 hour and after 24 hours, this reduction became statistically significant ($p = 0.018$). In addition to the observed reduction, flow cases typically showed a discontinuous distribution as seen in Figure 4a. (b) KLF2 expression appeared to be higher with flow, though only the 24 increase was significant ($p = 0.017$). Error bars are ± s.e.m., * indicates $p < 0.05$ and $n = 6$ or 7.

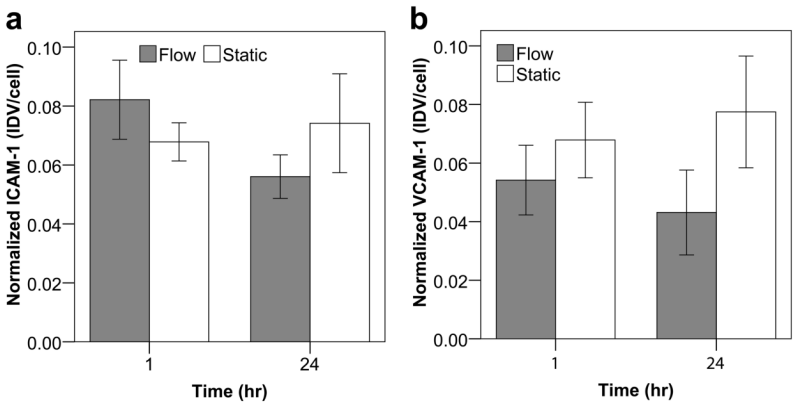

Figure 6.

Quantification of ICAM-1 (a) and VCAM-1 (b) expression on module surface through confocal microscopy and image analysis. The integrated density value (IDV) for ICAM-1 and VCAM-1 was normalized to the total number of visualized cells. No statistically significant differences in expression were found for ICAM-1 or VCAM-1 over the 24 hour time course. Though not statistically significant, ICAM-1 appeared to show a slight upregulation with flow after 1 hour followed by a downregulation after 24 hours (a). VCAM-1 results also suggested a marginal downregulaion with flow at both time points (b). Collectively, this data appears to verify our initial hypothesis that, unlike atherosclerotic-like disturbed flow, perfusion through the tortuous channels of the module bed does not significantly increase the amount of endothelial cell activation. Error bars are ± s.e.m. and n = 6, 7 or 8.

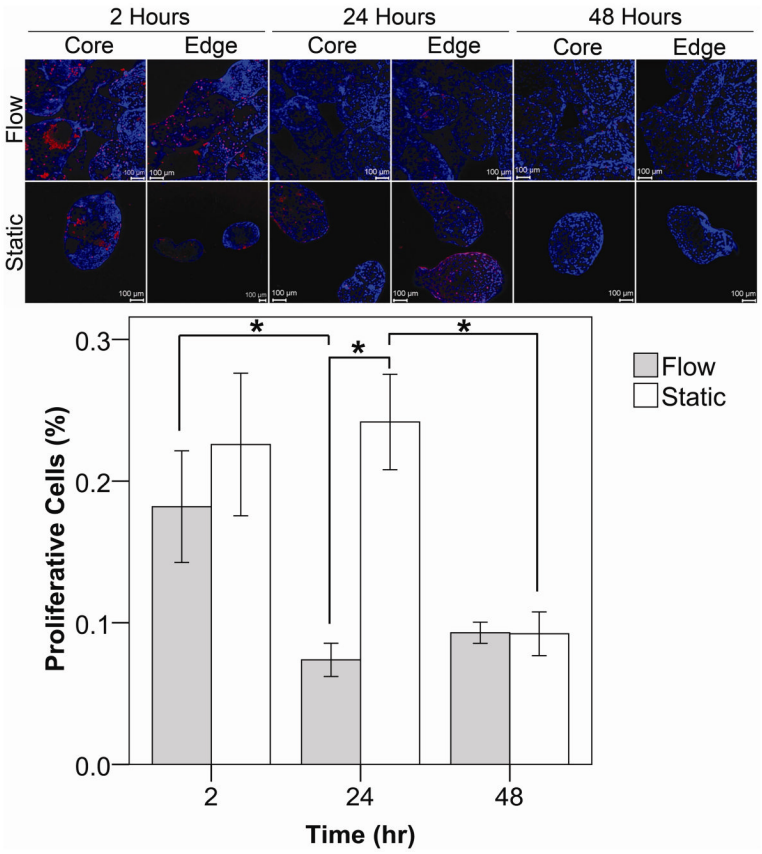

Figure 7.

Collagen modules with a confluent layer of HUVEC were subjected to flow (0.5 mL min^{-1}) for up to 2 days. Proliferating HUVEC incorporated BrdU into their DNA and appeared red. Nuclei were counterstained in blue. The entire packed module bed was examined for proliferation including the interior (core) and perimeter (edge), as indicated. After 2 hours, HUVEC proliferation was similar for both the flow and static cases. After 24 hours of flow, there was less proliferation present, as compared to static controls ($p < 0.001$) and the 2 hour flow case ($p = 0.010$). At the 48 hour mark, proliferation for both the static and flow cases became similar as the amount of proliferation in the static controls dropped from its 24 hour high ($p < 0.05$). Error bars are ± s.e.m.,* indicates $p < 0.05$ and n ranges between 5 and 14. Scale bars = 100 μm.